DR QIANG CHEN (Orcid ID : 0000-0002-2398-4482)

DR GUO-BO LI (Orcid ID : 0000-0002-4915-6677)

PROFESSOR YONG WU (Orcid ID : 0000-0003-0719-4963)

Article type : Research Article

Structure-based discovery of new selective small molecule sirtuin 5 inhibitors

Sha Liu[a,†], Sen Ji[a,†], Zhu-Jun Yu[a], Hua-Li Wang[a], Xu Cheng[a], Wei-Jian Li[a], Li Jing[a], Yamei Yu[a], Qiang Chen[a], Ling-Ling Yang[b], Guo-Bo Li[a,*], Yong Wu[a,*]

[a] *Key Laboratory of Drug Targeting and Drug Delivery System of Ministry of Education, West China School of Pharmacy, and Laboratory of Biotherapy and Cancer Center, West China Hospital, West China Medical School, Sichuan University, Chengdu 610041, China.*

[b] *College of Food and Bioengineering, Xihua University, Sichuan 610039, China*

[†]S. Liu and S. Ji contributed to equally this work.

[*]Corresponding author: liguobo@scu.edu.cn (G.-B. Li); wyong@scu.edu.cn (Y. Wu).

This article has been accepted for publication and undergone full peer review but has not been through the copyediting, typesetting, pagination and proofreading process, which may lead to differences between this version and the Version of Record. Please cite this article as doi: 10.1111/cbdd.13077

Abstract

Human sirtuin 5 (SIRT5) is a protein deacylase regulating metabolic pathways and stress responses, and is implicated in metabolism-related diseases. Small molecule inhibitors for SIRT5 are sought as chemical tools and potential therapeutics. Herein we proposed a customized virtual screening approach targeting catalytically important and unique residues Tyr102 and Arg105 of SIRT5. Of the 20 tested virtual screening hits, 6 compounds displayed marked inhibitory activities against SIRT5. For the hit compound **19**, a series of new synthesized (*E*)-2-cyano-N-phenyl-3-(5-phenylfuran-2-yl)acrylamide derivatives/analogues were carried out structure-activity relationship analyses, resulting in new more potent inhibitors, among which **37** displayed the most potent inhibition to SIRT5 with an IC_{50} value of 5.59 ± 0.75 μM. The biochemical studies revealed that **37** likely acts *via* competitive inhibition with the succinyl-lysine substrate, rather than the NAD^+ cofactor, and it manifested substantial selectivity for SIRT5 over SIRT2 and SIRT6. This study will aid further efforts to develop new selective SIRT5 inhibitors as tools and therapeutics.

Keywords: Sirtuins; Deacylase; SIRT5; Virtual screening; Structure-activity relationship (SAR)

Introduction

Sirtuins are nicotinamide adenine dinucleotide (NAD^+)-dependent lysine deacylases, which are highly conserved from bacteria to human.[1,2] There are seven human sirtuin isoforms, SIRT1-7, which are divided into four classes: SIRT1-3 belong to class I, SIRT4 to class II, SIRT5 to class III, and SIRT6-7 to class IV.[2] Originally, sirtuins were known as deacetylases acting on acetyl-lysine substrates from histones and non-histone proteins such as p53 and β-tubulin.[1,2] Recent studies revealed that sirtuins could remove other acyl groups, including propionyl,[3] butyryl,[3] malonyl,[4] glutaryl,[5] succinyl,[4] crotonyl,[6] and myristoyl [7] moieties. Although all sirtuins have a conserved catalytic core domain, they possess different deacylation activities other than deacetylation activity. For example, SIRT5 can catalyze desuccinylation, demalonylation and deglutarylation more efficiently than deacetylation,[4,5] whereas SIRT6 preferentially hydrolyzes long-chain fatty acyl groups, such as myristoyl-lysine residues.[7-9] SIRT4 can remove lipoic acid and biotin residues from active site lysines both *in vitro* and *in vivo*,[10] while SIRT1-3 seems to be decrotonylases.[6,8] Owing to the multifaceted activity on various substrate proteins, sirtuins are implicated in many biological processes such as metabolic regulation, transcriptional regulation, genome stability, and cell survival.[1,2,11-13]

SIRT5, which mainly localizes in the mitochondrial matrix and preferentially hydrolyzes acidic acyl modifications, was found to play a pivotal role in mitochondrial metabolism, e.g., amino acid degradation, the tricarboxylic acid cycle, and fatty acid metabolism.[14,15] Park *et al* recently revealed that SIRT5 represses biochemical activity of, and cellular respiration through pyruvate dehydrogenase complex (PDC) and succinate dehydrogenase (SDH)[14];

dysregulated PDC or SDH activity is linked to type 2 diabetes and cancer.[13,16-18] Another study showed that SIRT5 could positively regulate glycolysis *via* demalonylation of glycolytic enzymes, providing a possible link to cancer metabolism.[15,19] Lu *et al* found that SIRT5 is overexpressed in human non-small-cell lung cancer and associated with poor outcomes.[20] All of these studies indicate that SIRT5 is likely a potential molecular target for the treatment of metabolism-related disorders through interference with enzymes involved in metabolism pathways. Small molecule inhibitors for SIRT5 are thus sought as valuable chemical tools and potential therapeutics. However, currently almost all the reported SIRT5 inhibitors[21,22], such as nicotinamide, suramin, GW5074, sirtinol, cambinol, and thiobarbiturates (Supporting Information Figure S1), suffer from poor selectivity, particularly displaying inhibition against other sirtuin isoforms. Therefore, it is presently desirable to develop new selective SIRT5 inhibitors. In recent years, considerable efforts have been made to develop new virtual screening approaches,[23-26] which could substantially improve the efficiency of identifying new hit/lead compounds for SIRT5.

Superimposition of SIRT5 structure with other sirtuin isoforms reveals that SIRT5 has a similar overall domain organization and fold to SIRT1-3, but different with SIRT6 and SIRT7 (Supporting Information Figure S2); Tyr102 and Arg105 located in the catalytic core domain are the unique residues of SIRT5 (Supporting Information Figure S2a), which are important for specifically recognizing acidic acyl-lysine substrates.[4,27,28] We thus proposed a customized virtual screening method to screen the compounds that are likely to interact with Tyr102 and Arg105. We then used a fluorogenic small-molecule substrate to test the inhibitory activities against SIRT5 for the hit compounds from virtual screening.

Subsequently, we carried out structure-activity relationship studies for new synthesized (*E*)-2-cyano-N-phenyl-3-(5-phenylfuran-2-yl)acrylamide derivatives/analogues with aim of identifying new potent SIRT5 inhibitors. For the most potent inhibitor, we further examined the effects of NAD^+/substrate concentrations to the inhibitory potency and tested the selectivity to other sirtuin isoforms.

1. Results

1.1. Customized virtual screening.

Since Tyr102 and Arg105 are catalytically important and unique residues of SIRT5 (Supporting Information Figure S2), we developed a customized virtual screening method to search for compounds that are likely to specifically interact with Tyr102 and Arg105. In the virtual screening protocol, Autodock vina docking program[29] was first used to generate possible binding poses for the enquired compounds, followed by the use of protein-ligand interaction fingerprint (IFP)-based method[25,26] to filter the compounds potentially having hydrogen-bonding/electrostatic interactions with Tyr102 and Arg105 (Details see Experimental section). We employed this virtual screening protocol to screen against our *in-house* compound database that contains more than 15,000 small-molecule synthesized compounds. A total of 635 compounds were predicted with Vinascore lower than -6.5 kcal/mol and to have hydrogen-bonding/electrostatic interactions with Tyr102 and Arg105. These compounds were further inspected visually to check whether the predicted binding poses are reasonable and to select diverse compounds as potential SIRT5 inhibitors. Finally,

20 hit compounds (Figure 1) were selected for subsequent biochemical test; to the best of our knowledge, all of these compounds have not been reported as sirtuin inhibitors so far. The predicted binding modes of the selected compounds (**1**-**20**) are shown in Figure 1. We observed that although these compounds may have different binding modes with SIRT5, all of them are likely to form hydrogen-bonding/electrostatic interactions with Tyr102 and Arg105 (Figure 1).

1.2.In vitro inhibitory activities of virtual screening hits against SIRT5.

We then tested the inhibitory activities of the 20 selected hits from virtual screening against recombinant human SIRT5 proteins (Details regarding protein expression and purification see Experimental section) at 100 μM using a fluorogenic small-molecule substrate (SuBKA)-coupled trypsin assay[28] (Supporting Information Figure S3a) similar as that established by Jung *et al*[22]. The concentrations of NAD^+ and SuBKA used for the activity test are 200 μM and 10 μM, respectively. The results revealed that most of the 20 tested compounds displayed inhibition against SIRT5, and half of them had >30% inhibition (Table 1). Compounds **2**, **6**, **9**, **11**, **18**, and **19** manifested inhibition rates with 51.3% ± 5.5%, 61.3% ± 5.3%, 70.03% ± 0.56%, 77.26% ± 1.38%, 94.3% ± 0.53%, and 97.14% ± 1.03%, respectively (Table 1). We observed that the most potent compounds **18** and **19** displayed dose-dependent inhibitory activities to SIRT5 (Figure 2a-b), with IC_{50} values of 18.30 ± 0.88 μM and 9.26 ± 2.09 μM, respectively; both are more potent than the known SIRT5 inhibitor Nicotinamide (IC_{50} = 45.7 ± 7.42 μM, Figure 2c). Notably, **18** and **19** are predicted to have

similar binding modes with SIRT5 (Figure 1r and 1s); in particular, their carboxylate group is likely positioned to make hydrogen-bonding/electrostatic interactions with Tyr102 and Arg105 (Figure 1r and 1s). These results indicated the customized virtual screening method, which searched for compounds likely to interact with Tyr102 and Arg105, is a useful strategy for the identification of new SIRT5 inhibitors.

1.3.Structure-activity relationship studies.

With aim of identifying more potent SIRT5 inhibitor, we next synthesized new (*E*)-2-cyano-N-phenyl-3-(5-phenylfuran-2-yl)acrylamide (the core scaffold of compound **19**) derivatives/analogues with different amide-N-substituents (moiety **A**) and furan-5-substituents (moiety **B**) (compounds **21**-**39** in Table 2; $^{1}H/^{13}C$ NMR spectra of these compounds shown in Supporting Information Figure S6-S24) and carried out structure-activity relationship (SAR) analyses for these new synthesized compounds.

The route used for the synthesis of **21**-**39** are summarized in Scheme 1. The commercially available mono-substituted or poly-substituted aniline (**40**) was reacted with 2-cyanoacetic acid (**41**) in the presence of PCl_5 to give the substituted 2-cyano-N-phenylacetamide (**42**). Meanwhile, suzuki cross-coupling reactions of (5-formylfuran-2-yl)boronic acid (**43**) with substituted iodobenzene (**44**) led to the production of substituted 5-phenylfuran-2-carbaldehydes (**45**). Then, target compounds (**21-23**) and ester-containing intermediates were obtained by the condensation reactions between compounds **42** and **45** at

80 ℃ in the presence of piperidine as a catalyst. Finally, the ester-containing intermediates were directly converted to carboxyl-containing target compounds **24**-**39** *via* hydrolysis in the presence of NaOH at 60 ℃ for 0.5 h.

The inhibitory activities (IC_{50}) of **21**-**39** against SIRT5 are in Table 2. We observed that compounds **21**-**23**, with a moiety **A** of 3,4-dimethylbenzene and a moiety **B** of *p*-methylbenzoate (**21**), *p*-benzonitrile (**22**) or *p*-nitrobenzene (**23**), displayed lower inhibitory activities against SIRT5 than **25** (IC_{50} = 22.7 ± 2.61 μM, Table 2), which has a moiety **A** of 3,4-dimethylbenzene and a moiety **B** of *p*-benzoic acid. Compared with **25**, **24** (IC_{50} = 100.6 ± 8.98 μM), containing a moiety **B** of *m*-benzoic acid, also showed a weaker inhibitory potency to SIRT5. These results indicated that the *p*-benzoic acid as moiety **B** may provide important pharmacophore features for binding with SIRT5; as observed by molecular docking simulations, the carboxylate group of the *p*-benzoic acid moiety is likely to be positioned to interact with residues Tyr102 and Arg105. Compounds **26** and **27**, bearing substituted *p*-benzoic acid as moiety **B**, showed comparable or slight weaker inhibitory potency to SIRT5 (with IC_{50} of 23.6 ± 2.70 μM and 57.4 ± 19.21 μM, respectively, Table 2), indicating that substituents on the phenyl of the *p*-benzoic acid (moiety **B**) do not seem to be able to markedly improve the inhibitory activity. We thus reserved the *p*-benzoic acid as moiety **B**, and synthesized compounds **28**-**39** with various substituents as moiety **A**. We observed that compounds **28**-**34**, with C/N/O-containing substituents, showed varied inhibitory activities (IC_{50}) from 8.03 μM to 40.9 μM (Table 2), which are better than Nicotinamide (IC_{50} = 45.7 ± 7.42 μM, Figure 2c); **34** has relatively good inhibitory activity

with an IC_{50} value of 8.03 ± 0.70 μM, slightly better than the virtual screening hit compound **19** (IC_{50} = 9.26 ± 0.88 μM, Figure 2b). Interestingly, **35** (IC_{50} = 62.2 ± 7.44 μM) with an *m*-benzoic acid as moiety **A** displayed an obviously less activity compared with **34** (IC_{50} = 8.03 ± 0.70 μM). Compounds **36**-**39**, containing halo-substituted moiety **A**, showed a slight better inhibitory activity than compound **25** (IC_{50} = 22.7 ± 2.61 μM, Table 2), excepting compound **39** (IC_{50} = 37.9 ± 6.13 μM, Table 2). Notably, compound **37** bearing 2-fluorobenzonitrile as moiety **A** manifested an IC_{50} value of 5.59 ± 0.75 μM (Figure 3a), which is better than the hit compound **19** (Table 2). The molecular docking studies indicated that, similar to **19** (Figure 1s), the *p*-benzoic acid moiety of **37** likely forms hydrogen-bonding and electrostatic interactions with Tyr102 and Arg105, and the amide linkage makes hydrogen bonds with Leu227 and Tyr255 (Figure 3b); additionally, the fluorine of **37** seems have halogen-bonding interactions with Asn226 (Figure 3b). We further used the LEADOPT program[30] to predict the ADMET properties (a total of 12 kinds of ADMET properties involved in LEADOPT) for all of the synthesized compounds. The results showed that all of these compounds have ADMET score ≥ 9. Taken together, the SAR studies revealed that the *p*-benzoic acid as moiety **B** is likely to provide essential pharmacophore features to bind with SIRT5, and it is possible to improve the inhibitory potency *via* modifications of moiety **A**.

*1.4.Compound **37** likely acts as a succinyl-lysine substrate competitive inhibitor.*

For compound **37** (IC_{50} = 5.59 ± 0.75 μM, Figure 3a), we tested the inhibitory potency in the presence of 0.1% Triton X-100 to check whether it inhibits SIRT5 enzymes through colloid-like aggregations[31]. We observed that **37** has similar SIRT5 inhibitory activity in the presence and absence of 0.1% Triton X-100, probably excluding the possibility that **37** is a promiscuous aggregate. We next examined the effects of the concentrations of NAD^+ cofactor and SuBKA substrate (Supporting Information Figure S3a) on the inhibition potency of **37** against SIRT5. The results are shown in Figure 4a-b and Table 3. No obvious difference between inhibitory activities of **37** against SIRT5 for different concentrations of NAD^+ was observed (Figure 4a and Table 3), suggesting that **37** probably does not bind to the NAD^+ pocket, thereby having no competitive relationship with the NAD^+ cofactor. In contrast, we observed that the inhibition potency of **37** to SIRT5 is apparently affected by different concentrations of the SuBKA substrate (Figure 4b). When treated with 300 μM, 100 μM, 33 μM, and 11 μM of SuBKA, the inhibitory activities (IC_{50}) of **37** to SIRT5 are 28.35 ± 2.47 μM, 28.02 ± 2.02 μM, 14.93 ± 1.90 μM, and 6.64 ± 0.82 μM, respectively (Table 3), implying that **37** might be a SuBKA-competitive inhibitor of SIRT5. Comparison of the predicted binding mode of **37** with the crystal structure of SIRT5:sucH3K9 (PDB ID: 4F4U)[27] revealed that **37** likely has a similar binding mode with the peptide substrate sucH3K9 (Figure 4c); both have hydrogen-bonding interactions with Tyr102, Arg105, Leu227, and Tyr255, electrostatic interactions with Arg105, and hydrophobic interactions with Phe223 (Figure 4c). These results indicated that **37** likely mimics the sucH3K9 substrate and acts *via* competitive inhibition with the succinyl-lysine substrate of SIRT5.

*1.5. Compound **37** displayed no or very weak inhibitory activity against SIRT2 and SIRT6.*

With aim of examining the selectivity of compound **37** to other sirtuin isoforms, we next tested the inhibitory activity against class I enzyme SIRT2 and class IV enzyme SIRT6. The Benzyl-Lys(Acetyl)-AMC (AcBKA, Supporting Information Figure S3b) and Ac-TARK$_{my}$-AMC (Supporting Information Figure S3c) were used as substrates for SIRT2 and SIRT6, respectively (Details see Experimental section).[28] We observed that **37** displayed no inhibition against SIRT2 even at the highest concentration of 600 μM (Supporting Information Figure S4a). Similarly, no obvious inhibitory activity to SIRT6 was observed for **37** (Supporting Information Figure S4b). We performed molecular docking studies for **37** with SIRT2 and SIRT6. No key interactions between **37** and SIRT2 and SIRT6 were observed for top-ranking docking poses (Figure S5). The results indicated that **37** has a good selectivity for SIRT5 over SIRT2 and SIRT6.

2. Discussion

This work clearly revealed the potential of a customized virtual screening method targeting specific active site features for the identification of hit compounds for SIRT5. Coupled with the fluorogenic substrate-based assays, several new hit compounds were identified, among which the (*E*)-2-cyano-N-phenyl-3-(5-phenylfuran-2-yl)acrylamide compound **19** displayed most potent inhibition to SIRT5. The limited SAR studies revealed that it is possible to improve the potency of (*E*)-2-cyano-N-phenyl-3-(5-phenylfuran-2-yl)acrylamide inhibitors towards SIRT5. The SAR

studies also resulted in a potent SIRT5 inhibitor, compound **37**, with an IC_{50} value of 5.59 ± 0.75 μM. Further biochemical studies found that **37** likely acts as a succinyl-lysine substrate, rather than NAD^+, competitive inhibitor, and manifests substantial selectivity for SIRT5 over SIRT2 and SIRT6. Overall, this study provides an effective *in silico* approach for rapid identification of hit compounds for SIRT5, and will aid further efforts to develop new selective SIRT5 inhibitors as tools and therapeutics.

3. Experimental section

4.1. Virtual screening details. The customized virtual screening protocol employed molecular docking simulations and docking pose analyses, which are sequentially described below.

4.1.1 Docking simulations using AutoDock Vina. The in-house chemical database, containing more than 15,000 small-molecule compounds, was used as the screening database. The chemical structures (pdf format) were converted to mol2 format using OpenBabel [32], and then further converted to pdbqt format for AutoDock Vina [29] using the Raccoon script (http://autodock.scripps.edu/resources/raccoon).

An X-ray crystal structure of human SIRT5 in complex with a bicyclic intermediate (PDB ID: 4F56)[27] was used as the docking template. The bicyclic intermediate, water molecules, and other solvent molecules were removed. The protein model was then assigned with Gasteiger-Marsili charges and added non-polar hydrogens using AutoDockTools (http://autodock.scripps.edu/resources/adt). The binding site was set as a square grid. The

grid center was set to coordinates of [x, y, z = -7.85, -3.03, 14.21] and the grid size was set to 23Å × 23Å × 23Å encompassing the entire SIRT5 catalytic core domain. The number of docking poses was set as 10, and the other parameters for Vina were set as default.

4.1.2 Docking pose analyses. With the aim of searching for compounds likely to interact with catalytic important residues Tyr102 and Arg105, we carried out docking poses analyses using an interaction fingerprint (IFP)-based method. The IFP method involves eight types of protein-ligand interactions, including hydrogen-bond donor, hydrogen-bond acceptor, positively charge, negatively charge, face-to-face π-π stacking interactions, edge-to-face π-π stacking interactions, and hydrophobic interactions as that in our previously reported methods[26,30,33,34]. In this study, we filtered the compounds that potentially form hydrogen-bonding and electrostatic interactions (negatively charges) with Tyr102 and Arg105. The filtered compounds were further inspected visually to check whether the predicted docking poses are reasonable and to select structurally diverse compounds. To the end, a total of 20 compounds were selected and tested against SIRT5 activity *in vitro* (see Table 1); all these compounds (purity: >98%) were purchased from Enamine Ltd and used without further purification.

4.2. Protein cloning, expression, and purification. The human SIRT5 (residues 34-269) were PCR-amplified and cloned into the PET28 vector resulting in a construct with N-terminal His-tag and a TEV protease cleavage site. Proteins were expressed in *E. coli* Transetta(DE3) cells overnight at 16 ℃, and induced for overexpression using isopropyl β-D-1-thiogalactopyranoside (IPTG, 0.3 mM final concentration) at an OD_{600} of 0.6~0.8. The

cells were harvested and resuspended in lysis buffer(20 mM Tris–HCl, 250 mM NaCl, pH 8.0), and then lysed by a ultrahigh-pressure homogenizer. The cellular debris was removed by centrifugation at 15,000 r/min for 30 min. The supernatant was applied onto an Ni-NTA column (Roche), followed by extensive washing with 20 volumes of 20 mM Tris-HCl pH 8.0, 250 mM NaCl with 10 mM imidazole to remove nonspecifically binding proteins. Recombinant proteins were eluted with 20 mM Tris-HCl pH 8.0, 250 mM NaCl with 250 mM imidazole, and then further exchanged to the buffer of 50 mM Tris-HCl pH 8.0, 150 mM NaCl. The resulted SIRT5 proteins were pooled and concentrated to ~10 mg/ml and stored at -80 °C. All purification steps were monitored by SDS-PAGE and the concentration was determined by NannoDrop 2000 spectro photometer (Thermo Scientific). Human $SIRT2_{25\text{-}389}$ and $SIRT6_{1\text{-}355}$ proteins were purified similarly as described above.

4.3. Fluorescence-based inhibition assays. The inhibition activities of compounds against recombinant human SIRT5 were performed with a fluorescence-based assay similar as that established by Jung *et al*[22,28]. The fluorogenic substrate Benzyl-Lys(Succinyl)-AMC (SuBKA, Supporting Information Figure S3a) was used. All the enzymes and substrates were dissolved in the assay buffer: 50 mM Tris, 137 mM NaCl, 2.7 mM KCl, pH 8.0. The assay was performed in 96-well black microplate (Corning No. 3603) with a reaction volume of 60 μL per well. Reaction wells contained SIRT5 proteins (0.2 μM), SuBKA (10 μM), NAD^+ (200 μM), and/or the compounds at different concentrations. Control wells containing SuBKA, NAD^+, and/or compounds (with the same concentrations as that in reaction wells) in assay buffer were included in each plate with aim of excluding the interference of fluorescent compounds. The reactions were incubated for 2 h at 37 ℃ and 140 rpm, and then stopped by

the addition of 60 μL of a solution containing 3~4 $U \cdot \mu L^{-1}$ trypsin (Sigma-Aldrich No. T8003) and 8 mM nicotinamide, followed by further incubation for 20 min at 37 ℃ and 140 rpm. Fluorescence intensity was measured using a microplate reader (BioTek Cytation 3, λ_{ex} = 390 nm, λ_{em} = 460 nm). The IC_{50} determination was performed with compound concentrations varying from 600 μM to 0.03 μM in 3-fold dilution. All determinations were performed in triplicates. The inhibition rate was calculated using the formula: $Inh\% = 100 - \frac{F_{ac}-F_c}{F_a-F_0} \times 100$, where F_{ac} denotes fluorescence in a reaction well containing compounds, F_a denotes fluorescence in a reaction well without compounds, F_c denotes fluorescence in a control well containing compounds, and F_0 denotes fluorescence in a control well without compounds. The IC_{50} values were obtained using Graphpad Prism software (La Jolla, CA).

4.3.1 NAD^+/substrate competitive assay. To investigate the inhibition mechanism of **37** against SIRT5, we tested the effects of varied concentrations of SuBKA or NAD^+ to the inhibition potency. With different concentrations of NAD^+ (800 μM, 400 μM, 200 μM, 100 μM, and 50 μM), the IC_{50} values were tested under the conditions of SIRT5 (0.2 μM), SuBKA (200 μM) and **37** (600 μM ~ 0.03 μM). When treated with different concentrations of SuBKA (300 μM, 100 μM, 33 μM, and 11 μM), the IC_{50} values were obtained with SIRT5 (0.2 μM), NAD^+ (200 μM) and **37** (600 μM ~ 0.03 μM).

4.3.2 Selectivity against SIRT2 and SIRT6. With aim of examining the selectivity to other sirtuin isoforms, **37** was tested against SIRT2 and SIRT6. The substrates Benzyl-Lys(Acetyl)-AMC (AcBKA, Supporting Information Figure S3b) and Ac-$TARK_{my}$-AMC (Supporting Information Figure S3c) were used for SIRT2 and SIRT6 activity test, respectively. The SIRT2 proteins (0.5 μM) were mixed with AcBKA (20 μM),

NAD^+ (200 μM) or/and different concentrations of **37** (600 μM ~ 0.03 μM). The SIRT6 proteins (0.2 μM) were mixed with Ac-$TARK_{my}$-AMC (10 μM), NAD^+ (200 μM) or/and different concentrations of **37** (600 μM ~ 0.03 μM). The activity test methods for SIRT2 and SIRT6 are similar with that described above for SIRT5.

4.4. Chemical synthesis. All the reagents were purchased from market (e.g., Sigma-Aldrich agency, Shanghai, China; Juhui Chemical, Chengdu, China) and were used without further purification. Reactions were monitored by thin layer chromatography (TLC) on Merck silica gel 60 F-254 thin layer plates. All the target compounds were purified to >95% purity, as determined by high-performance liquid chromatography (HPLC). HPLC analysis was performed on a Waters 2695 HPLC system equipped with a Kromasil C18 column (4.6 mm × 250 mm, 5 μm). ^{1}H NMR and ^{13}C NMR spectra were recorded on a Bruker AV-400 spectrometer at 400 MHz and 100 MHz, respectively. Chemical shifts (δ) are quoted in parts per million (ppm) relative to tetramethylsilane (TMS) as an internal standard. Low-resolution and high-resolution mass spectral (MS) data were acquired on an Agilent 1100 series LC-MS instrument with UV detection at 254 nm in electrospray ionization (ESI) mode.

General procedure 1: PCl_5-mediated amide formation. To a cooled solution of 2-cyanoacetic acid (**41**, 1.0g, 11.7 mmol) in dichloromethane (20 ml), phosphorus pentachloride (PCl_5, 2.5g, 12 mmol) was slowly added. The reaction mixture was stirred at 40 ℃ for 0.5 h, and then substituted anilines (11.5 mmol) were added to the reaction at room temperature. Subsequently, the mixture was warmed to 40℃ and stirred for 2h. Upon

completion of the reaction as determined by TLC, the organic solvent was concentrated to dryness and the residue was dispersed into 50 ml ice water. At this time, a brown solid was formed and collected by filtration. The crude product was washed by saturated $NaHCO_3$ (10 ml) and anhydrous ether (20 ml) to give substitued 2-cyano-N-phenylacetamide (**42**, 80-92%). These products were taken up for the next step without any purification.

General procedure 2: Suzuki cross-coupling reaction. A mixture of (5-formylfuran-2-yl)boronic acid (**43**, 1.5 equiv), substituted iodobenzene (**44**, 1.0 equiv), Na_2CO_3 (2.0 equiv) and $Pd(PPh_3)_2Cl_2$ (0.1 equiv) in MeCN/H_2O (5 mL/ 1 mmol) was stirred at 60℃ for 1.0 h under a nitrogen atmosphere. Upon completion of the reaction as determined by TLC, the mixture was filtered and the filtrate was concentrated *in vacuo*. The products were purified by column chromatography with appropriate eluents (PE/EA). Yield: 67-88%.

General procedure 3: Piperidine-mediated condensation reaction reaction. To a solution of substitued 2-cyano-N-phenylacetamides (**42**, 1.0 equiv) substitued 5-phenylfuran-2-carbaldehydes (**45**, 1.0 equiv) in EtOH (5ml/1.0mmol), catalytic amount of piperidine was added. Then the reaction was allowed to warm to 80 ℃ and stirred for 2 h. After completion (monitored by TLC), the mixture was concentrated under reduced pressure. The residues were purified by column chromatography with appropriate eluents (PE/EA) to give target compound **21**-**23** and ester-containing intermediates. Yield: 75-92%.

General procedure 4: Hydrolytic reaction of ester. The ester-containing intermediates (1.0 equiv) were taken in THF/MeOH (6 mL/mmol), and NaOH (1.0 equiv) was added. The

reaction mixture was refluxed for ~0.5 h at 60 ℃. After completion (monitored by TLC), the mixture was concentrated and acidified with 1 M HCl (pH 4-5). During the acidification, a buff solid was formed and collected by filtration. The filter cake was washed with a small amount of water and dried in a vacuum oven to give the product **24**-**39**. Yield: 65-78%.

ACKNOWLEDGEMENTS

This work was supported by the National Natural Science Foundation of China (Grant No. 81502989 and 81373259), the Scientific Research Foundation of Sichuan University (Grant No. 20822041A4193), and the China Postdoctoral Science Foundation Funded Project (Grant No. 2015M570789).

CONFLICT OF INTEREST

The authors declare no conflict of interest.

SUPPORTING INFORMATION

Additional Supporting Information may be found online in the supporting information tab for this article.

Figure Legends

Figure 1. (a-t) The predicted binding modes of the hit compounds **1**-**20**. Compounds are shown in green sticks and dash lines represent hydrogen-bonding interactions.

Figure 2. (a-b) The inhibitory activity (IC_{50}) curves of the virtual screening hits **18** and **19**, and (c) the known SIRT5 inhibitor Nicotinamide.

Figure 3. (a) The inhibitory activity (IC_{50}) curves of **37** against SIRT5. (b) View of the predicted binding mode of **37** with SIRT5.

Figure 4. (a-b) The inhibitory activity (IC50) curves of **37** against SIRT5 obtained with different concentrations of NAD+ cofactor and SuBKA substrate. (c) Superimposition of the predicted binding mode of **37** with the crystal structure of SIRT5:sucH3K9 (PDB ID: 4F4U)[27] reveals that **37** has a similar binding mode with sucH3K9.

Scheme 1. Reagents and conditions: (a) PCl_5, CH_2Cl_2, 40℃, 2h; (b) substituted iodobenzene, Na_2CO_3, $Pd(PPh_3)_2Cl_2$, MeCN:H_2O=1:1, 60℃, 1h; (c) Piperidine, EtOH, 80℃, 2h; (d) NaOH, THF/MeOH, 60℃, 0.5h.

References

[1] B. Chen, W. Zang, J. Wang, Y. Huang, Y. He, L. Yan, J. Liu, W. Zheng, *Chem. Soc. Rev.* **2015**, *44*, 5246.

[2] R. H. Houtkooper, E. Pirinen, J. Auwerx, *Nat. Rev. Mol. Cell Biol.* **2012**, *13*, 225.

[3] Y. Chen, R. Sprung, Y. Tang, H. Ball, B. Sangras, S. C. Kim, J. R. Falck, J. Peng, W. Gu, Y. Zhao, *Mol. Cell. Proteomics* **2007**, *6*, 812.

[4] J. Du, Y. Zhou, X. Su, J. J. Yu, S. Khan, H. Jiang, J. Kim, J. Woo, J. H. Kim, B. H. Choi, B. He, W. Chen, S. Zhang, R. A. Cerione, J. Auwerx, Q. Hao, H. Lin, *Science* **2011**, *334*, 806.

[5] M. Tan, C. Peng, Kristin A. Anderson, P. Chhoy, Z. Xie, L. Dai, J. Park, Y. Chen, H. Huang, Y. Zhang, J. Ro, Gregory R. Wagner, Michelle F. Green, Andreas S. Madsen, J. Schmiesing, Brett S. Peterson, G. Xu, Olga R. Ilkayeva, Michael J. Muehlbauer, T. Braulke, C. Mühlhausen, Donald S. Backos, Christian A. Olsen, Peter J. McGuire, Scott D. Pletcher, David B. Lombard, Matthew D. Hirschey, Y. Zhao, *Cell Metab.* **2014**, *19*, 605.

[6] X. Bao, Y. Wang, X. Li, X.-M. Li, Z. Liu, T. Yang, C. F. Wong, J. Zhang, Q. Hao, X. D. Li, *eLife*. **2014**, *3*, e02999.

[7] X. Zhang, S. Khan, H. Jiang, M. A. Antonyak, X. Chen, N. A. Spiegelman, J. H. Shrimp, R. A. Cerione, H. Lin, *Nat. Chem. Biol.* **2016**, *12*, 614.

[8] J. L. Feldman, J. Baeza, J. M. Denu, *J. Biol. Chem.* **2013**, *288*, 31350.

[9] H. Jiang, S. Khan, Y. Wang, G. Charron, B. He, C. Sebastian, J. Du, R. Kim, E. Ge, R. Mostoslavsky, H. C. Hang, Q. Hao, H. Lin, *Nature* **2013**, *496*, 110.

[10] Rommel A. Mathias, Todd M. Greco, A. Oberstein, Hanna G. Budayeva, R. Chakrabarti, Elizabeth A. Rowland, Y. Kang, T. Shenk, Ileana M. Cristea, *Cell* **2014**, *159*, 1615.

[11] M. S. Bonkowski, D. A. Sinclair, *Nat. Rev. Mol. Cell Biol.* **2016**, *17*, 679.

[12] L. Yang, X. Ma, C. Yuan, Y. He, L. Li, S. Fang, W. Xia, T. He, S. Qian, Z. Xu, G. Li, Z. Wang, *Eur. J. Med. Chem.* **2017**, *134*, 230.

[13] S. Xu, C.-X. Liu, W. Xu, L. Huang, J.-Y. Zhao, S.-M. Zhao, *Signal Transduct. Target. Ther.* **2017**, *2*, 16035.

[14] J. Park, Y. Chen, D. X. Tishkoff, C. Peng, M. Tan, L. Dai, Z. Xie, Y. Zhang, B. M. Zwaans, M. E. Skinner, D. B. Lombard, Y. Zhao, *Mol. Cell* **2013**, *50*, 919.

[15] Y. Nishida, Matthew J. Rardin, C. Carrico, W. He, Alexandria K. Sahu, P. Gut, R. Najjar, M. Fitch, M. Hellerstein, Bradford W. Gibson, E. Verdin, *Mol. Cell* **2015**, *59*, 321.

[16] M. A. Selak, S. M. Armour, E. D. MacKenzie, H. Boulahbel, D. G. Watson, K. D. Mansfield, Y. Pan, M. C. Simon, C. B. Thompson, E. Gottlieb, *Cancer Cell* **2005**, *7*, 77.

[17] A. M. Cervera, J. P. Bayley, P. Devilee, K. J. McCreath, *Mol. Cancer* **2009**, *8*, 89.

[18] E. H. Smith, R. Janknecht, L. J. Maher, 3rd, *Hum. Mol. Genet.* **2007**, *16*, 3136.

[19] A. Chalkiadaki, L. Guarente, *Nat. Rev. Cancer* **2015**, *15*, 608.

[20] W. Lu, Y. Zuo, Y. Feng, M. Zhang, *Tumour Biol.* **2014**, *35*, 10699.

[21] L. Yang, X. Ma, Y. He, C. Yuan, Q. Chen, G. Li, X. Chen, *Sci. China Life Sci.* **2017**, *60*, 249.

[22] B. Maurer, T. Rumpf, M. Scharfe, D. A. Stolfa, M. L. Schmitt, W. He, E. Verdin, W. Sippl, M. Jung, *ACS Med. Chem. Lett.* **2012**, *3*, 1050.

[23] E. Cichero, P. D'Ursi, M. Moscatelli, O. Bruno, A. Orro, C. Rotolo, L. Milanesi, P. Fossa, *Chem. Biol. Drug Des.* **2013**, *82*, 718.

[24] E. Cichero, S. Espinoza, S. Franchini, S. Guariento, L. Brasili, R. R. Gainetdinov, P. Fossa, *Chem. Biol. Drug Des.* **2014**, *84*, 712.

[25] G.-B. Li, L.-L. Yang, Y. Yuan, J. Zou, Y. Cao, S.-Y. Yang, R. Xiang, M. Xiang, *Methods* **2015**, *71*, 158.

[26] G.-B. Li, M. I. Abboud, J. Brem, H. Someya, C. T. Lohans, S.-Y. Yang, J. Spencer, D. W. Wareham, M. A. McDonough, C. J. Schofield, *Chem. Sci.* **2017**, *8*, 928.

[27] Y. Zhou, H. Zhang, B. He, J. Du, H. Lin, R. A. Cerione, Q. Hao, *J. Biol. Chem.* **2012**, *287*, 28307.

[28] H.-L. Wang, S. Liu, Z.-J. Yu, C. Wu, L. Cheng, Y. Wang, K. Chen, S. Zhou, Q. Chen, Y. Yu, G.-B. Li, *RSC Adv.* **2017**, Accepted

[29] O. Trott, A. J. Olson, *J. Comput. Chem.* **2010**, *31*, 455.

[30] G.-B. Li, S. Ji, L.-L. Yang, R.-J. Zhang, K. Chen, L. Zhong, S. Ma, S.-Y. Yang, *Eur. J. Med. Chem.* **2015**, *93*, 523.

[31] B. Y. Feng, A. Shelat, T. N. Doman, R. K. Guy, B. K. Shoichet, *Nat. Chem. Biol.* **2005**, *1*, 146.

[32] N. M. O'Boyle, M. Banck, C. A. James, C. Morley, T. Vandermeersch, G. R. Hutchison, *J. Cheminformatics* **2011**, *3*, 33.

[33] G.-B. Li, L.-L. Yang, W.-J. Wang, L.-L. Li, S.-Y. Yang, *J. Chem. Inf. Model.* **2013**, *53*, 592.

[34] G.-B. Li, L.-Y. Huang, H. Li, S. Ji, L.-L. Li, S.-Y. Yang, *RSC Adv.* **2016**, *6*, 61137.

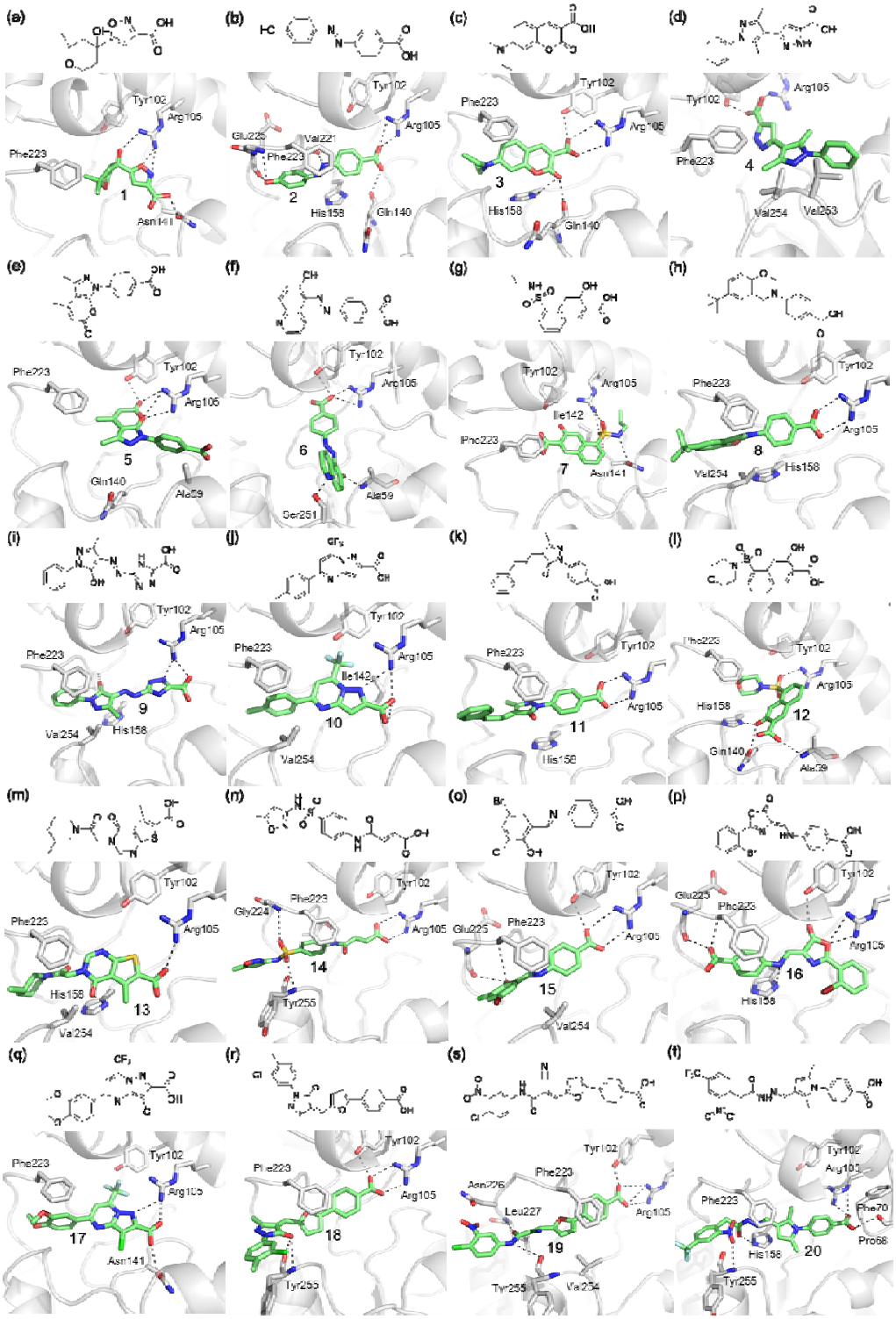

Figure 1. (a-t) The predicted binding modes of the hit compounds **1**-**20**. Compounds are shown in green sticks and dash lines represent hydrogen-bonding interactions.

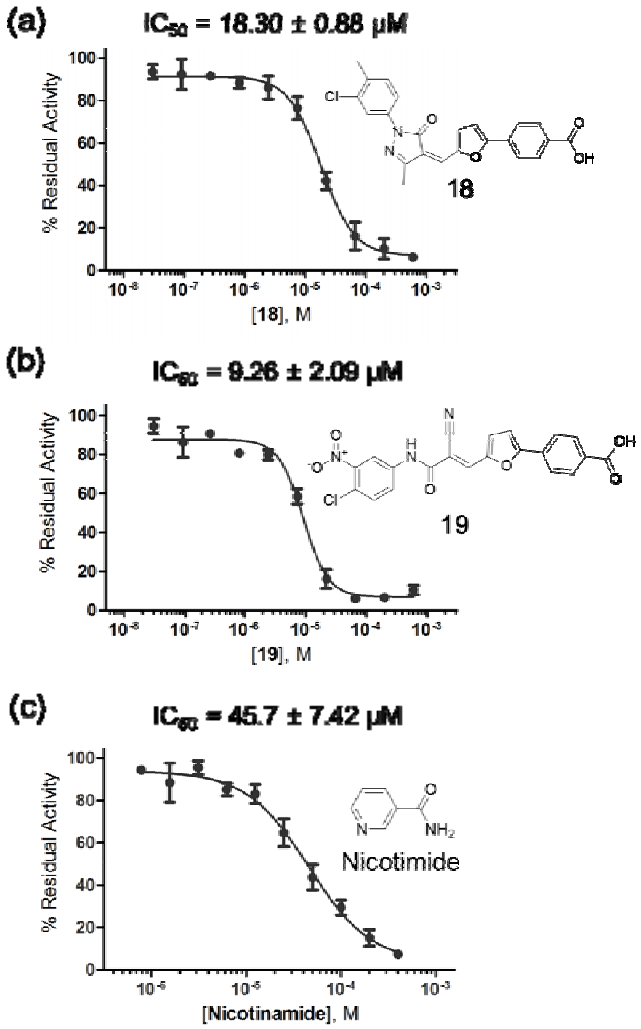

Figure 2. (a-b) The inhibitory activity (IC_{50}) curves of the virtual screening hits **18** and **19**, and (c) the known SIRT5 inhibitor Nicotinamide.

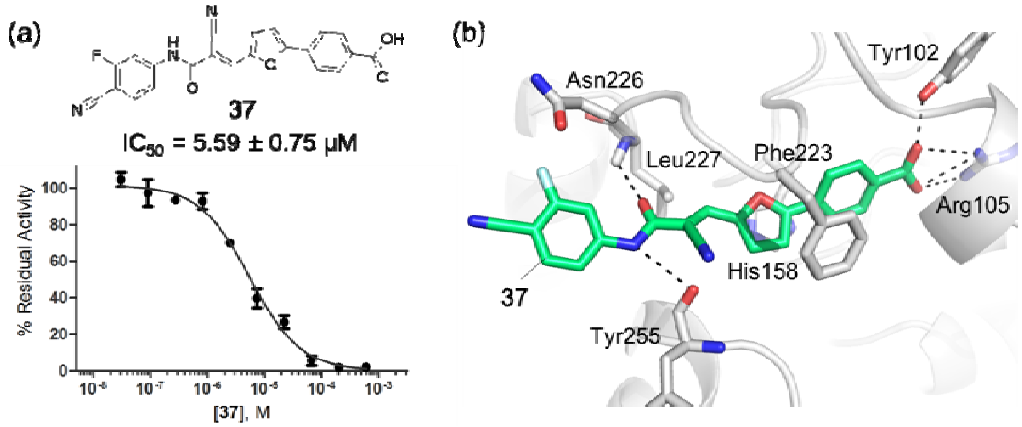

Figure 3. (a) The inhibitory activity (IC_{50}) curves of **37** against SIRT5. (b) View of the predicted binding mode of **37** with SIRT5.

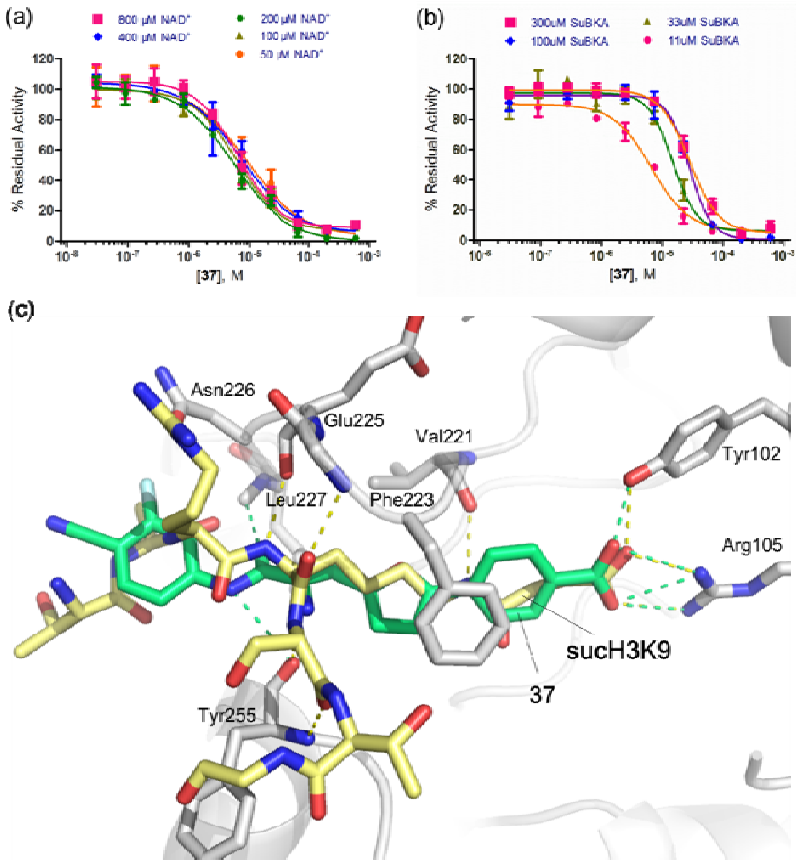

Figure 4. (a-b) The inhibitory activity (IC_{50}) curves of **37** against SIRT5 obtained with different concentrations of NAD^+ cofactor and SuBKA substrate. (c) Superimposition of the predicted binding mode of **37** with the crystal structure of SIRT5:sucH3K9 (PDB ID: 4F4U)[27] reveals that **37** has a similar binding mode with sucH3K9.

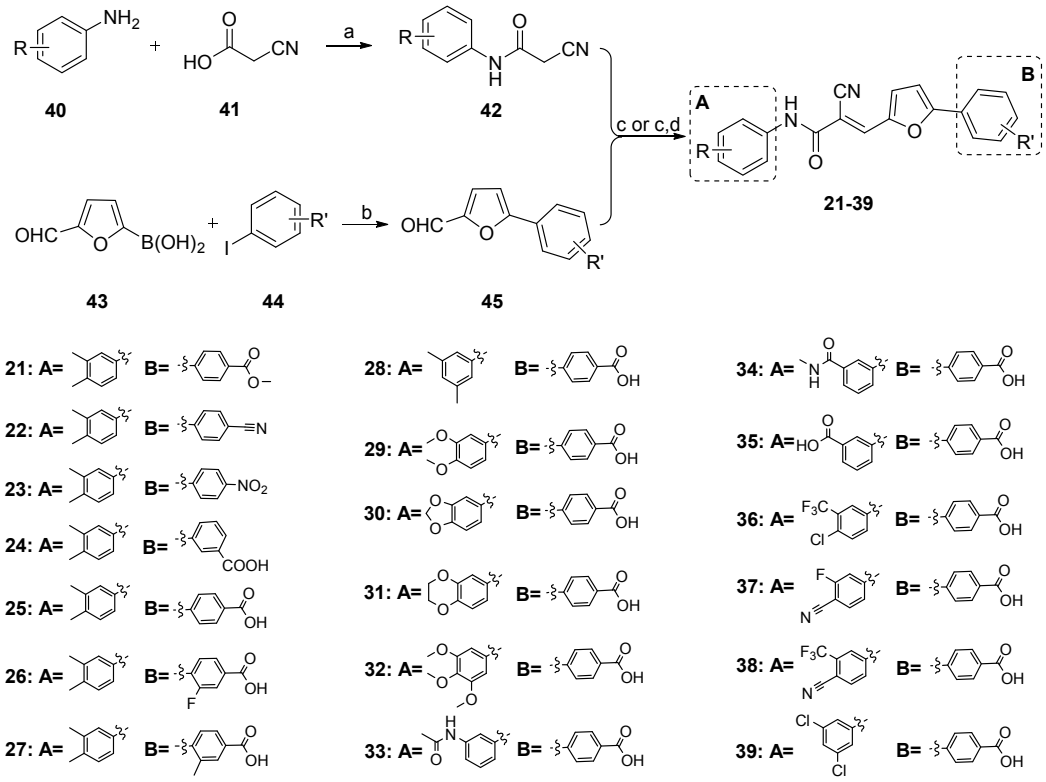

Scheme 1. Reagents and conditions: (a) PCl_5, CH_2Cl_2, 40℃, 2h; (b) substituted iodobenzene, Na_2CO_3, $Pd(PPh_3)_2Cl_2$, MeCN:H_2O=1:1, 60℃, 1h; (c) Piperidine, EtOH, 80℃, 2h; (d) NaOH, THF/MeOH, 60℃, 0.5h.

Table 1. Chemical structures and inhibitory activities of the 20 hit compounds identified by customized virtual screening.

Cpd. ID	M. W.	Chemical Structure	Inh%@100μM
1	241.24	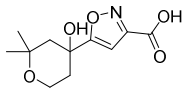	17.41 ± 13.83
2	242.23	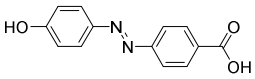	51.3 ± 5.5
3	261.28	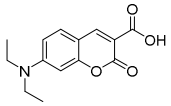	28.91 ± 24.12
4	282.30	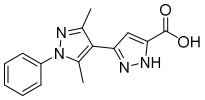	21.54 ± 10.87
5	284.27	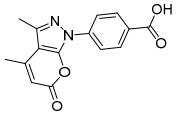	18.70 ± 12.73
6	293.28	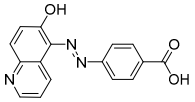	61.3 ± 5.3
7	307.32	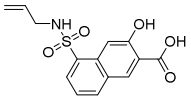	17.43 ± 1.82
8	311.38	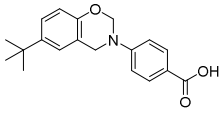	24.54 ± 1.93
9	313.28	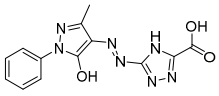	70.03 ± 0.56
10	321.26	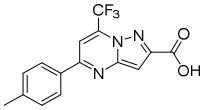	11.08 ± 11.2
11	332.36	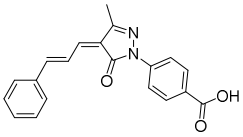	77.26 ± 1.38
12	337.35	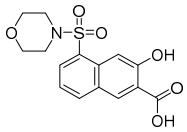	9.2 ± 3.80
13	349.41	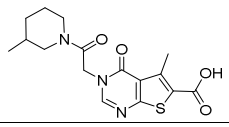	15.43 ± 2.23

14	351.33	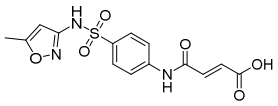	-5.54 ± 1.37
15	354.58	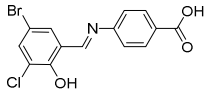	33.66 ± 8.07
16	387.19	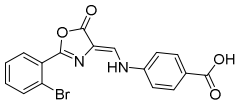	34.24 ± 14.39
17	401.73	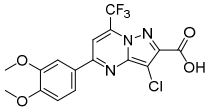	30.85 ± 2.33
18	420.85	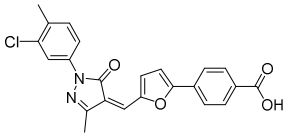	94.3 ± 0.53
19	437.79	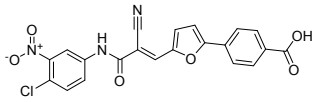	97.14 ± 1.03
20	488.42	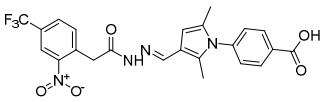	73.75 ± 8.91
Nicotinamide	122.13	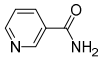	70.57 ± 5.68

Table 2. The inhibitory activities (IC_{50}) of new (*E*)-2-cyano-N-phenyl-3-(5-phenylfuran-2-yl)acrylamide derivatives/analogues against SIRT5. s

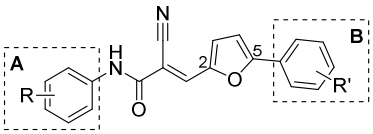

Cpd. ID	Moiety **A**	Moiety **B**	IC_{50} (μM)	ADMET score[a]
19	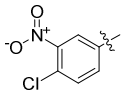	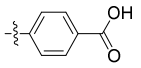	9.26 ± 0.83	9
21		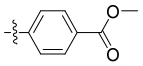	133.4 ± 34.32	9
22		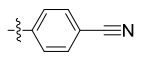	82.7 ± 32.23	9
23		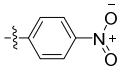	72.1 ± 7.83	9
24		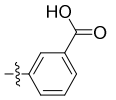	100.6 ± 8.98	10
25		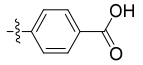	22.7 ± 2.61	9
26		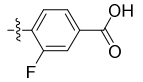	23.6 ± 2.70	10
27		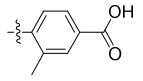	57.4 ± 19.21	9
28		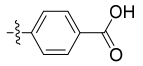	40.9 ± 5.91	9
29	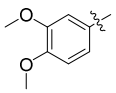	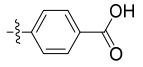	36.9 ± 6.98	10
30	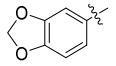	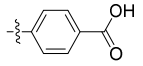	10.8 ± 1.62	10
31	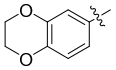	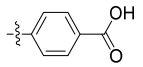	32.3 ± 3.33	9
32	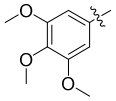	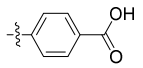	24.3 ± 5.93	10

33	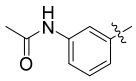	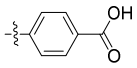	18.0 ± 2.04	10
34	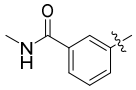	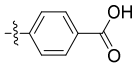	8.03 ± 0.70	10
35	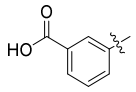	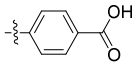	62.2 ± 7.44	10
36	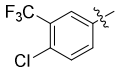	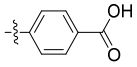	16.4 ± 1.81	10
37	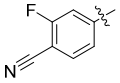	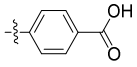	5.59 ± 0.75	10
38	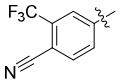	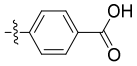	13.9 ± 1.57	10
39	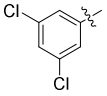	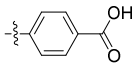	37.9 ± 6.13	9
Nicotinamide		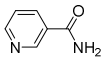	45.7 ± 7.42	6

[a] The ADMET score is calculated using the LEADOPT program,[30] which involves 12 important ADMET properties including human oral bioavailability, caco-2 cell permeability, in vivo clearance, human intestine absorption, human plasma protein binding rate, pregnane X receptor ligand, half lethal concentration, aqueous solubility, mitochondria toxicity, genotoxicity, human ether-a-go-go-related gene toxicity, and teratogenicity.

Table 3. The inhibitory activities (IC_{50}) of compound **37** against SIRT5 with different concentrations of NAD^+ or SuBKA.

NAD^+/SuBKA	Concentration (μM)	IC_{50} (μM)
NAD^+	800	6.27 ± 1.06
	400	7.17 ± 1.65
	200	5.59 ± 0.75
	100	6.18 ± 0.80
	50	8.66 ± 2.27
SuBKA	300	28.35 ± 2.47
	100	28.02 ± 2.02
	33	14.93 ± 1.90
	11	6.64 ± 0.82